3D kinetic Monte Carlo-based investigation of the influence of dopants on the reliability of VCM ReRAM

N. Kopperberg (10); D. Genua Noguera; S. Menzel 22 (10)



J. Appl. Phys. 137, 175105 (2025) https://doi.org/10.1063/5.0262843





Articles You May Be Interested In

Zeolitic-imidazolate framework (ZIF-67) based bipolar memristor for nonvolatile ReRAM application

Appl. Phys. Lett. (June 2024)

A nanoscale analysis method to reveal oxygen exchange between environment, oxide, and electrodes in ReRAM devices

APL Mater. (November 2021)

Accurate evaluation method for HRS retention of VCM ReRAM

APL Mater. (March 2024)







3D kinetic Monte Carlo-based investigation of the influence of dopants on the reliability of VCM ReRAM

Cite as: J. Appl. Phys. 137, 175105 (2025); doi: 10.1063/5.0262843 Submitted: 3 February 2025 · Accepted: 14 April 2025 · Published Online: 2 May 2025







N. Kopperberg, D. Genua Noguera, and S. Menzel^{2,a)}

AFFILIATIONS

- ¹Institut für Werkstoffe der Elektrotechnik II (IWE2), RWTH Aachen University, 52074 Aachen, Germany
- ²Peter-Grünberg-Institut 7 (PGI-7), Forschungszentrum Jülich GmbH, 52425 Jülich, Germany

ABSTRACT

Variability and retention are critical reliability challenges for redox-based resistive switching random access memory (ReRAM) devices operating via the valence change mechanism (VCM). Variability arises from stochastic oxygen vacancy dynamics at short timescales, while retention failure manifests itself by the long-term instability of the programmed states. Both challenges become more severe in large-scale memory arrays, requiring a better understanding of the mechanisms and effective optimization strategies. In this work, we employ an advanced 3D Kinetic Monte Carlo simulation model to systematically investigate the influence of dopants on these reliability issues. For variability, we demonstrate that dopants significantly enhance the signal-to-noise ratio by stabilizing oxygen vacancy dynamics through a trapping effect, which reduces the frequency of current fluctuations. For retention, we show that dopants improve the stability of current distributions over time, where they effectively suppress distribution broadening and slow mean current degradation. Our simulation results 🚊 provide valuable insights into optimizing the reliability of VCM ReRAM via dopants for practical applications. While these findings align with existing experimental data, the scope of experimental studies on doped VCM ReRAM devices remains limited, particularly concerning large-scale statistics and short-term variability. Therefore, our simulations not only corroborate previous experimental observations but also highlight the need for further experimental investigations to enhance the performance of VCM ReRAM devices for next-generation memory applications.

© 2025 Author(s). All article content, except where otherwise noted, is licensed under a Creative Commons Attribution (CC BY) license (https://creativecommons.org/licenses/by/4.0/). https://doi.org/10.1063/5.0262843

I. INTRODUCTION

The increasing demand for non-volatile memories (NVMs), driven by advancing digitization in various aspects of everyday life, has significantly expanded research into emerging memory technologies.^{1,2} Among these, redox-based resistive switching random access memory (ReRAM) is a promising candidate to replace Flash, which is nearing its physical limits.³⁻⁵ While early research focused on fundamental mechanisms, memristive technologies have now advanced significantly and are being explored for a wide range of real-world applications, as discussed in recent reviews of the field.^{3,6,7} This high industrial interest underlines the importance of understanding and optimizing reliability aspects, such as variability and retention.^{8,9} ReRAM offers several advantages, including fast switching speeds down to 20 ps, 10,11 high scalability with

sub-10 nm² cells, 12,13 and low operating voltages (< 2 V). 14,15 Additionally, its potential for neuromorphic computing applications has further increased interest in this technology.

Bipolar switching valence change mechanism (VCM)-based ReRAM cells have been extensively studied due to their promising characteristics. These devices typically consist of a transition metaloxide layer sandwiched between two metal electrodes: an electronically active electrode (AE) with a high work function and an ohmic electrode (OE) with a low work function. 17,18 By applying external voltages, oxygen vacancies-mobile ionic defects within the oxide—are generated during an initial electroforming step, creating a conductive filament through the oxide layer. 19,20 The filament can then be ruptured by moving oxygen vacancies away from the AE, forming a depletion zone or gap, and subsequently

a) Author to whom correspondence should be addressed: st.menzel@fz-juelich.de

reconstructed depending on the polarity of the applied voltage. This process allows the cell to switch between a high resistive state (HRS) and a low resistive state (LRS), enabling data storage. These states can be read out non-destructively by applying a small read

As VCM ReRAM devices approach commercial deployment, reliability has become a critical focus.^{9,22} Among the key reliability aspects, variability, retention, and endurance are of particular importance, as all three are strongly influenced by the stochastic behavior of oxygen vacancies. Variability presents a significant challenge for consistent device performance. Random movements of oxygen vacancies during forming, SET, RESET, read processes, and even at rest lead to fluctuations in resistance states, switching voltages, and timing parameters, complicating the development of reliable memory arrays.²³ Retention refers to the ability of a ReRAM cell to maintain its programmed resistance state over extended periods. Long-term retention is hindered by the diffusion and recombination of oxygen vacancies, which can destabilize the conductive filament or the depletion region. This process directly impacts the ability of devices to meet the stringent requirements of applications, such as automotive or industrial memory systems.²⁴ Endurance, defined as the maximum number of reliable switching cycles, is another critical factor. Repeated switching gradually affects the material properties of the active region, primarily through the generation and redistribution of oxygen vacancies, leading to eventual failure in the form of hard breakdown or stuck states.^{25,26} To overcome these challenges, it is essential to develop effective methods for minimizing variability, enhancing retention, and improving endurance to ensure the long-term reliability of VCM ReRAM devices in practical applications.

Despite the limited number of studies investigating the impact of dopants on the reliability of VCM ReRAM devices, the existing research provides highly promising results. These studies highlight the potential of dopants to enhance key reliability aspects by stabilizing the conductive filament and modulating oxygen vacancy behavior. A comprehensive investigation was conducted by Kempen et al.,27 who demonstrated that zirconium (Zr) doping in TaOx-based ReRAM devices significantly improves retention and endurance. Their experiments showed that Zr-doped devices achieved more than a 50-fold increase in endurance, sustaining up to 2.9×10^{10} switching cycles compared to 4.5×10^8 cycles in undoped devices. Additionally, the doped devices maintained stable memory states significantly longer at temperatures up to 320°, attributed to an increased diffusion barrier for oxygen vacancies induced by doping. Chen et al.28 provided complementary evidence, showing that dopants raise the activation energy for oxygen vacancy migration, thereby improving retention stability at elevated temperatures. Similarly, He *et al.*²⁹ highlighted the ability of dopants to reduce resistance fluctuations and stabilize the filament structure, further enhancing retention performance under hightemperature conditions. Jiang and Stewart³⁰ employed density functional theory (DFT) calculations to systematically investigate the impact of various metal dopants on oxygen vacancy formation in Ta₂O₅-based ReRAM. Their results indicate that p-type dopants can reduce the forming voltage and suggest that dopant-induced vacancy stabilization may enhance filament stability, potentially improving device variability and retention. Schie et al.31 used

atomistic simulations to show that acceptor-type dopants in SrTiO₃ influence oxygen vacancy migration beyond the nearest-neighbor approximation. Their results suggest that long-range dopantvacancy interactions could affect both filament stability and variability in resistive switching devices. While the effects of dopants on retention and endurance have been explored in these few experimental studies introduced before, the impact on variability remains largely underexamined. Zhao et al. 32 addressed this gap through DFT simulations, showing that weak p-type or n-type dopants reduce the formation energy of oxygen vacancies and mitigate their stochastic behavior. These findings suggest that dopants can significantly reduce variability in resistance states by stabilizing the conductive filament. However, no experimental investigations into the role of dopants on variability have been reported, leaving a critical gap in the literature.

The promising experimental findings from the literature provide a strong motivation for further investigation into the role of dopants in VCM ReRAM devices. While the studies by Kempen et al.,27 Chen et al.,28 and He et al.29 demonstrate significant improvements in retention and endurance through doping, several critical aspects remain unexplored. A deeper understanding of the mechanisms behind the observed enhancements is essential, particularly to determine how specific dopants influence oxygen vacancy behavior and filament stability. Additionally, the impact of dopants on variability represents a major open question. Zhao et al. 32 highlighted the potential of dopants to reduce variability through computational simulations, but no experimental investigations or detailed statistical evaluations of variability have been conducted to scale memory arrays, it is imperative to systematically study how dopants affect the stochastic behavior of Furthermore, the findings from the literature are limited to results from single devices or averaged measurements. While these approaches provide valuable initial insights, they fail to capture the statistical nature of variability and other reliability metrics across multiple devices. To address these gaps, this work focuses on employing advanced simulation techniques to systematically investigate the influence of dopants on variability and retention in VCM ReRAM devices.

In this work, dopants were incorporated into an existing and validated 3D Kinetic Monte Carlo (KMC) model^{33–35} to study their impact on the reliability of VCM ReRAM devices. The enhanced model allows for a detailed investigation of how dopants influence key reliability aspects, particularly variability and retention. By simulating the stochastic behavior of oxygen vacancies under the influence of dopants, this study demonstrates the potential of doping to significantly reduce variability and improve retention stability, providing valuable insights for optimizing ReRAM performance.

II. SIMULATION

A. 3D KMC model

To investigate the influence of dopants on the reliability of VCM ReRAM devices, an advanced 3D Kinetic Monte Carlo (KMC) model was employed. This model is based on previous works by Kopperberg et al. 33,34 and Abbaspour and captures the stochastic behavior of oxygen vacancies within the oxide layer. The

simulated structure consists of a cubic lattice representing a (6 nm)³ HfO_x layer with a lattice spacing of 0.5 nm, sandwiched between a high work-function active electrode (AE) and a low work-function ohmic electrode (OE). The chosen lattice spacing of 0.5 nm corresponds to the typical scale of the atomic lattice constant in transition metal oxides, such as HfO_x, and thus reasonably matches the effective spatial extent of individual oxygen vacancies, which are treated as point defects within the simulation.³⁷ Furthermore, oxygen vacancies, the key defects responsible for conduction, can be distributed across the lattice points.

The local potential is determined by solving the Poisson equation, accounting for the applied voltage and the spatial charge distribution. Current through the device is calculated using a trap-assisted tunneling (TAT) mechanism, predominantly appropriate for the low oxygen vacancy concentrations in the high resistive state (HRS). Transition rates for oxygen vacancy generation, recombination, and diffusion are calculated based on Boltzmann statistics, and a weighted random selection governs the execution of these processes. Random numbers are drawn from a uniform distribution and used for event selection via standard inverse transform sampling, ensuring that the physical transition probabilities are correctly represented. The model inherently captures the statistical variability arising from the stochastic dynamics of oxygen vacancies, focussing on the diffusion processes that play the major role regarding variability as shown in previous works.

The model has been extended in this work to incorporate the effects of dopants on oxygen vacancy dynamics. Dopants are randomly distributed within the oxide layer, mimicking experimental conditions. Each dopant modifies the local energy landscape, introducing variations in the energy barriers for oxygen vacancy diffusion. The energy barriers for oxygen vacancy hopping into and out of dopant sites are adjusted by ΔE_{dop} , which depends on the dopant's relative position. This modification is incorporated into the transition rate calculation as follows:

$$R_{\rm D} = \nu_0 \exp\left(-\frac{E_{\rm D} - q\Delta\Phi + \Delta E_{\rm dop}}{k_{\rm B}T}\right),\tag{1}$$

where v_0 is the attempt frequency, E_D is the activation energy for diffusion, q is the oxygen vacancy charge, $\Delta\Phi$ is the local potential difference, and ΔE_{dop} represents the dopant-induced modification to the barrier. The dopants implemented in this work were specifically chosen to ensure a negative ΔE_{dop} , as this condition is expected to create a stabilizing effect on the conductive filament by reducing the overall mobility of oxygen vacancies. As illustrated in Fig. 1, dopants with negative ΔE_{dop} that are chosen in this work lower the diffusion barrier for oxygen vacancies hopping toward them, while increasing it for hopping away. This asymmetry stabilizes the oxygen vacancy configuration, promoting filament stability and reducing stochastic fluctuations. In contrast, the use of other dopants leading to a positive $\Delta E_{\rm dop}$ would likely worsen device reliability, as previously suggested by Zhao $et~al.^{32}$ In experimental and theoretical studies, dopants, such as Zr in TaOx, ²⁷ or Al, Si, and Ti in HfO₂, ^{28,30} have been shown to increase the activation energy for oxygen vacancy migration, thereby stabilizing device operation. Conversely, Zhao et al. 32 demonstrated that certain weak p- or

n-type dopants can reduce this barrier, potentially increasing variability. These findings motivate the parameter space explored in

Diffusion-limiting domains, previously implemented in the model,33 remain an essential component for capturing the subdiffusive behavior of oxygen vacancies in the oxide layer. These domains introduce spatially varying diffusion barriers, with higher barriers ($E'_{\rm D} = 1.2\,{\rm eV}$) at domain boundaries and lower barriers $(E_{\rm D}=0.7\,{\rm eV})$ within the domains. The addition of dopants complements this feature by further modulating local diffusion rates, providing a detailed framework for simulating key reliability aspects of VCM ReRAM. By integrating dopants into the simulation, the extended 3D KMC model allows for a systematic investigation of their effects on retention and variability.

The simulations were executed on the JURECA-DC cluster at Forschungszentrum Jülich using 128-core CPU nodes (2.25 GHz, 512 GB RAM).³⁸ Retention simulations typically required up to 24 h per run, executed in parallel (five simulations per node), while read simulations for variability investigations were significantly faster, taking approximately 4 h per run.

B. Results

To evaluate the impact of dopants on the reliability of VCM ReRAM devices, the second effects on two critical reliability metrics: value of Variability, which refers to fluctuations in the device's resistance states during read operations, is analyzed through dynamic read noise simulations. Retention, the ability of the device to maintain the programmed resistance state over extended periods, is investigated under accelerated lifetime testing (ALT) conditions.

1. Variability

The effect of dopants on the variability of VCM ReRAM devices is investigated using the 3D KMC simulation model introduced before. Variability is analyzed by simulating the dynamic read noise of cells programmed into the high resistive state (HRS), following the methodology established in previous studies.^{33,35} A set number of cells is initially programmed into the HRS by randomly placing a fixed amount of oxygen vacancies in a predefined filament $(2 \times 2 \times 3 \text{ nm}^3, 50 \text{ oxygen vacancies})$ and gap (5 additional oxygen vacancies) volume between the filament and AE. In the same volume of the filament and gap, a certain number of dopants with a certain $\Delta E_{\rm dop}$ value are also placed randomly. In these simulations, the time evolution of the read current under a constant read voltage of $V_{\rm read} = 0.35\,\mathrm{V}$ applied to the AE is monitored for a duration of t = 2 s. Typical current traces of undoped cells, as previously presented in Refs. 33 and 35 show no significant visual differences, even with the introduction of dopants into the oxide layer as presented in Fig. S1 of the supplementary material. This lack of observable differences motivates the use of a quantitative metric to assess variability.

To provide such a quantitative evaluation, the signal-to-noise ratio (SNR) is employed, following the definition by Voigtman³ and Schnieders et al. 40 The SNR quantifies the ratio of the mean

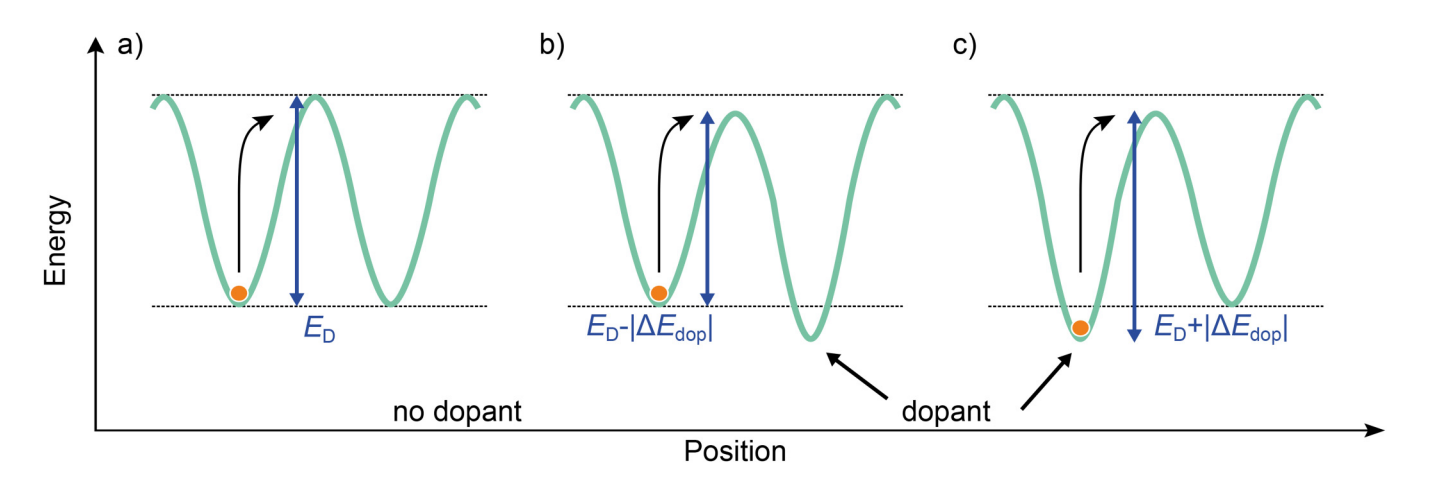


FIG. 1. Schematic illustration of the diffusion barrier modulation due to dopants. (a) Diffusion of oxygen vacancies (orange) to a neighboring site without dopants. (b) Lowered diffusion barrier for hopping toward a dopant. (c) Increased diffusion barrier for hopping away from a dopant. The dopants implemented in this work were specifically chosen to ensure a negative ΔE_{dop} , promoting filament stability and reducing stochastic fluctuations.

read current $\mu(I_{\text{read}})$ to the variability of the current noise $\sigma(I_{\text{noise}})$,

$$SNR_{avg} = \frac{\mu(I_{read})}{\sigma(I_{noise})},$$
 (2)

where $I_{\text{noise}}(t)$ is defined as the deviation of the read current $I_{\text{read}}(t)$ from its mean value,

$$I_{\text{noise}}(t) = I_{\text{read}}(t) - \mu(I_{\text{read}}). \tag{3}$$

The SNR is particularly important for VCM ReRAM applications in memory arrays, where low variability is essential to ensure uniform switching behavior across multiple devices. High SNR values directly translate to more reliable read operations and reduced error rates in large-scale integration scenarios.

The results of the SNR evaluation for various dopant concentrations and energy levels are presented in Fig. 2. Each matrix element corresponds to the average SNR for 30 simulated current traces. The SNR clearly improves (increases) with an increasing number of dopants and a decreasing dopant energy level. This indicates that dopants significantly reduce variability, with the number of dopants having a stronger effect within the investigated parameter range. An alternative definition of the SNR worst-case-scenario (SNR_{wc}) and the corresponding data evaluation for this parameter are presented in Fig. S2 of the supplementary material.

To understand the mechanism behind the improved SNR, the influence of dopants on the mean jump height of the current signal is analyzed. Figure 3(a) shows the dependence of the mean jump height on the dopant number, whereas Fig. 3(b) presents the dependence on the dopant energy level. In both cases, no significant dependence is observed, suggesting that dopants do not alter the type of oxygen vacancy-induced current fluctuations. In a previous study, we showed that the height of the jumps in the current signal can be assigned to certain jump types of the oxygen vacancies. 41 The type of jumps and their occurrence ratio do not seem to be influenced by dopants.

In contrast, the mean time between successive oxygen vacancy-induced current jumps shows a clear dependence on both parameters. Figure 4(a) illustrates that increasing the number of dopants leads to a stronger-than-linear increase in the mean jump time. Similarly, decreasing the dopant energy level significantly increases the mean jump time, as shown in Fig. 4(b), until saturation occurs at lower energy levels. These results indicate that 8 dopants with negative ΔE_{dop} act as traps for oxygen vacancies, $\frac{\sigma}{2}$ reducing their mobility and therefore lowering the frequency of $\frac{\sigma}{2}$ current fluctuations.

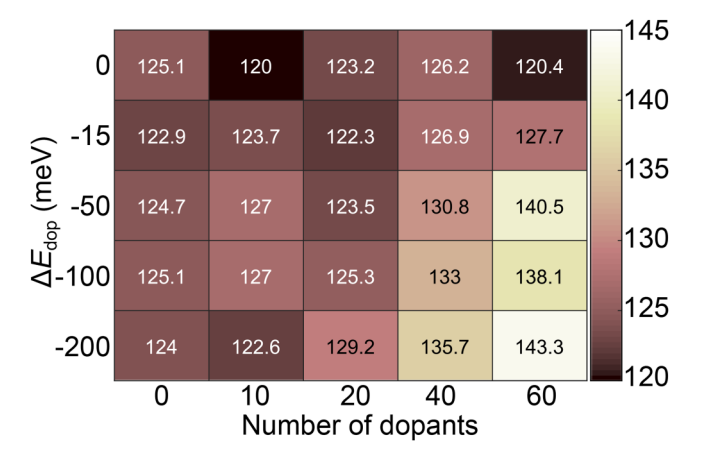


FIG. 2. Average signal-to-noise ratio SNR_{avg} for simulated read current traces of 30 cells for each matrix element under different dopant concentrations and energy levels ΔE_{dop} . Higher numbers of dopants and lower dopant energy levels significantly improve SNR_{avg} (brighter color), reducing variability.

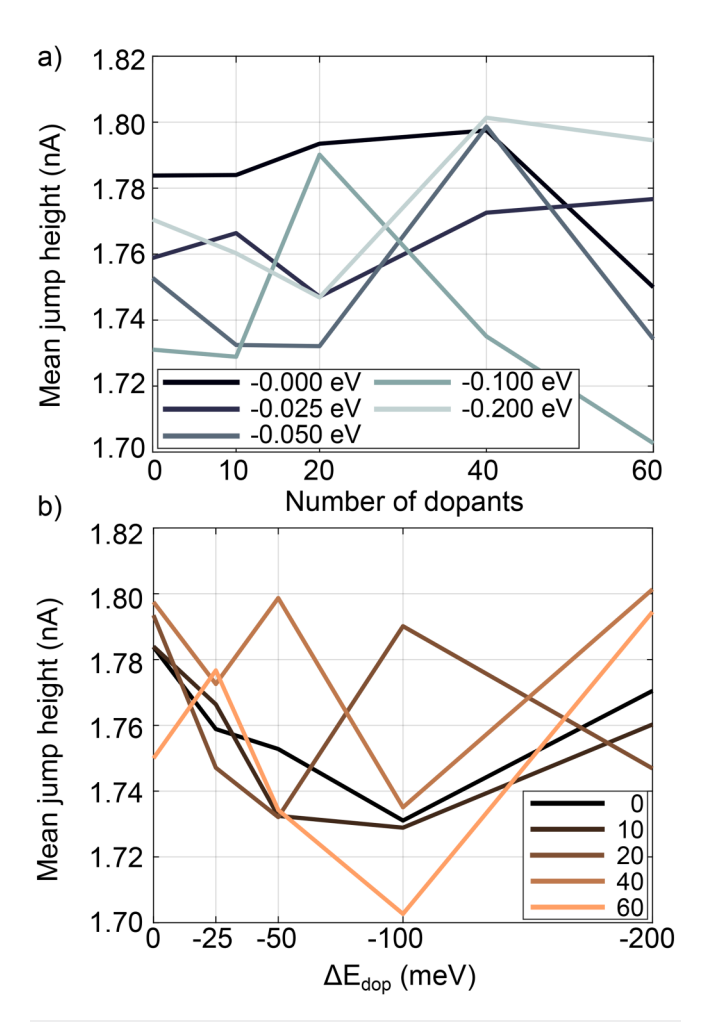


FIG. 3. Mean current jump height dependence during read operation. (a) Influence of the dopant number on the mean current jump height, evaluated for various dopant energy levels. No significant dependence of the jump height on the number of dopants can be observed. (b) Influence of the dopant energy level on the mean current jump height for different dopant numbers. Again, no notable influence of the energy level on the current jump height is observed.

In summary, the introduction of dopants into the oxide layer significantly reduces the variability of VCM ReRAM devices. The improved SNR is primarily attributed to the trapping effect of dopants, which reduces the frequency of oxygen vacancy-induced current fluctuations without altering their type. These findings demonstrate the potential of dopants to enhance the reliability of VCM ReRAM devices by stabilizing variability, which represents a strong motivation for future experimental investigations into the optimization of variability by appropriate doping.

2. Retention

The impact of dopants on the retention behavior of VCM ReRAM devices is investigated using the 3D KMC simulation

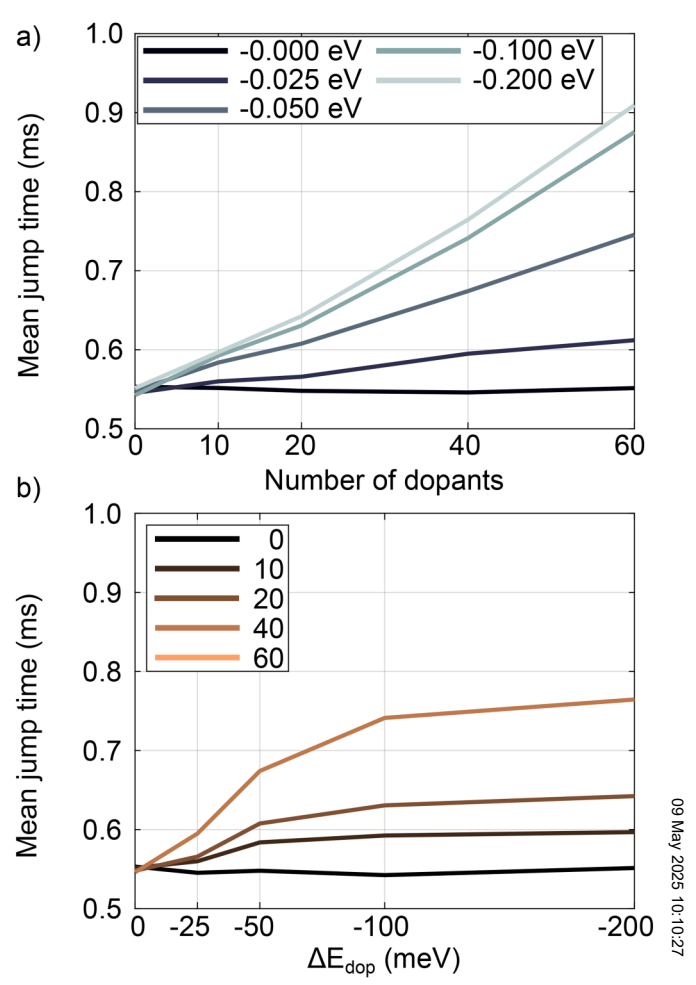


FIG. 4. Dependence of the mean time between successive oxygen vacancy-induced current jumps during read operation. (a) Influence of the dopant number on the mean time for different dopant energy levels. A strong increase in the jump time is observed with increasing dopant numbers. (b) Influence of the dopant energy level on the mean time for different dopant numbers. Lower energy levels result in a significant increase in the mean jump time until saturation occurs.

model. To evaluate the retention behavior of VCM ReRAM devices, accelerated lifetime testing (ALT) simulations are conducted at an elevated temperature of 1000 K. This approach significantly reduces simulation times, as retention processes at lower, application-relevant temperatures would require prohibitively long computation times. The methodology has been thoroughly motivated and validated in previous studies, 33,34 where ALT simulations yielded results that aligned well with experimental data. These findings confirm that ALT simulations provide a reliable and efficient means to study long-term retention effects in VCM ReRAM devices. The analysis in this study focuses on both the mean current and the distribution of read currents over time to evaluate the stability of the programmed state.

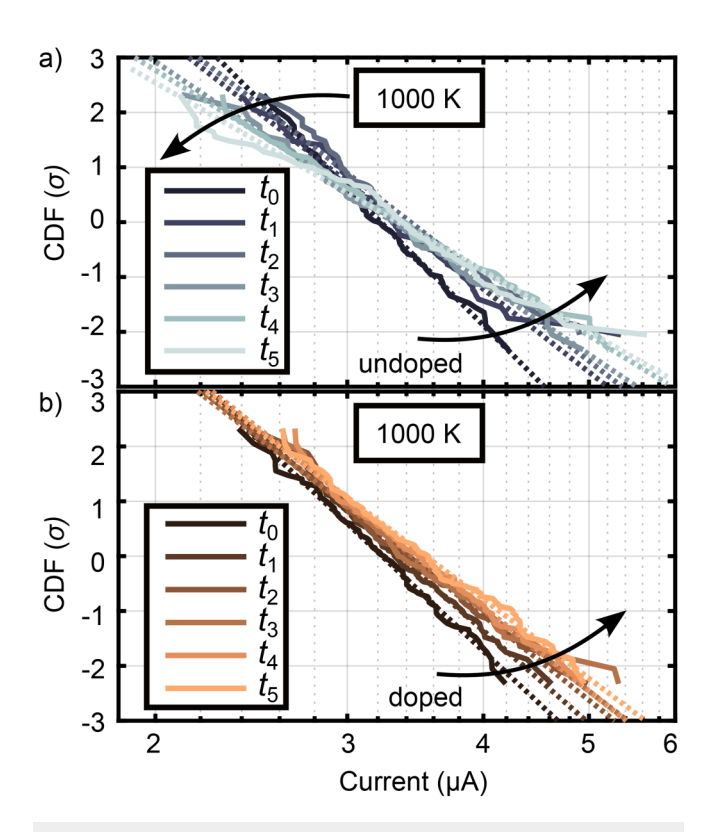


FIG. 5. Current distribution evolution over time at elevated temperatures (1000 K) for each 100 cells programmed to HRS. (a) Undoped devices show significant broadening of the current distribution represented by a tilt of the linear fit (dotted line). (b) In contrast, doped devices (60 dopants with $\Delta E_{\text{dop}} = -200 \,\text{meV}$) exhibit much more stable behavior over time.

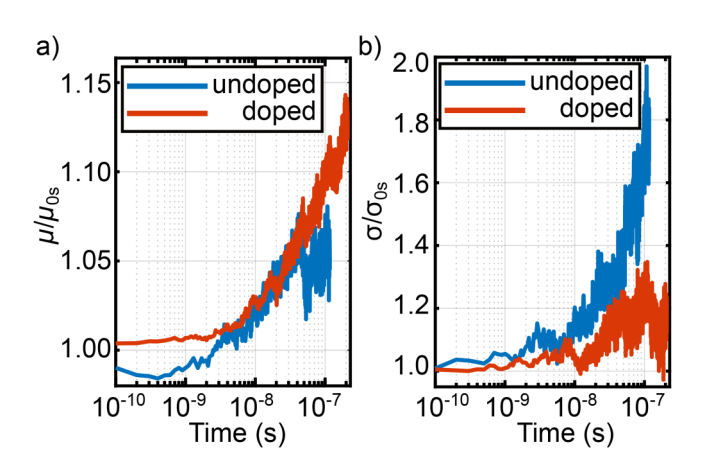


FIG. 6. Quantification of the current distribution over time for HRS cells. (a) The mean current slightly increases for both undoped and doped cells. A minimal higher trend to higher currents can be observed for the doped devices. (b) The standard deviation shows significant stabilization in doped cells compared to undoped devices.

To maximize the observable effect of the dopants, the simulations use the most promising parameter set identified in the variability study, with 60 dopants randomly distributed in the filament and gap region and a dopant energy level of $\Delta E_{\rm dop} = -200\,{\rm meV}.$ As before, the focus of investigations at this point is on cells that are programmed into an HRS as described in Sec. II B 1.

Figure 5 shows the evolution of the current distribution over time for 100 undoped and 100 doped cells. In undoped devices [Fig. 5(a)], the current distribution widens significantly over time, indicating a higher degree of variability as the retention degrades. In contrast, doped cells [Fig. 5(b)] exhibit much more stable current distributions, with only minimal broadening over time. In our previous work, 33 we identified the random movement of oxygen vacancies as the main reason for the long-term retention failure of the programmed states. In simple terms, the behavior can be divided into two main processes: the radial diffusion of oxygen vacancies out of the filament, which leads to a reduction in current, and the vertical diffusion from the filament into the gap volume, which leads to an increase in current. In the case shown here without dopants, both processes are well-balanced, so that the distribution mainly tilts and thus becomes broader. By introducing the dopants, the overall oxygen vacancy movements are reduced or

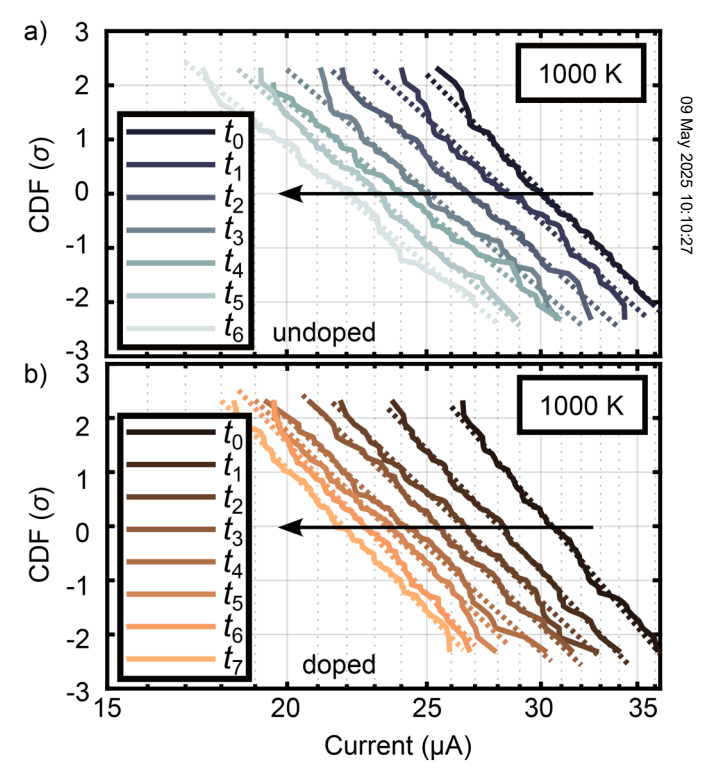


FIG. 7. Current distribution evolution over time at elevated temperatures (1000 K) for cells initially programmed to the LRS. (a) Undoped devices and (b) doped devices exhibit a similar shift of the distribution to lower currents over



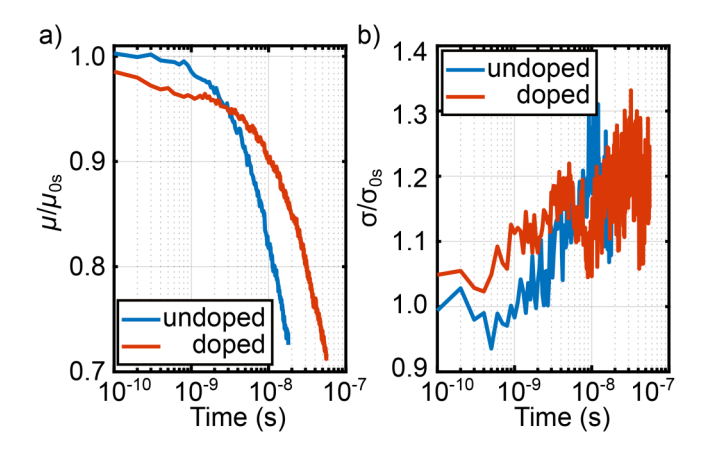


FIG. 8. Quantification of the current distribution over time for LRS cells. (a) The mean current decreases more slowly in doped devices, while (b) the standard deviation remains similar for both undoped and doped cells.

slowed down. In addition, the balance here seems to shift slightly toward processes that increase the current.

These observations are further quantified in Fig. 6, which presents the evolution of the mean current [Fig. 6(a)] and the standard deviation of the current distribution [Fig. 6(b)] that can be calculated as the inverse slope of the current distributions. While the mean current shows a slight increase for both cases, the standard deviation behaves differently: for undoped cells, the standard deviation increases significantly over time, reflecting degraded retention, whereas doped cells maintain a stable standard deviation, highlighting the positive effect of doping. Since, as we discussed in a previous work,³³ cells programmed into the HRS can show different retention behavior, we extended our investigations to HRS distributions where a shift predominates over a tilt during ALT. The corresponding results can be found in Fig. S3 of the supplementary material and also show the positive influence of dopants on the retention behavior.

Figure 7 extends the retention analysis to low resistive state (LRS) devices. For this purpose, a filament of dimensions $3 \times 4 \times 4$ nm³ with 172 randomly positioned oxygen vacancies is utilized. Similar to the HRS analysis, ALT simulations are conducted at 1000 K. The current distributions of undoped and doped cells show minimal visual differences, as both distributions shift toward lower currents over time.

However, the mean current of doped cells decreases more slowly over time compared to undoped devices [Fig. 8(a)], indicating improved retention performance. Notably, the standard deviation [Fig. 8(b)] shows no significant difference between doped and undoped cells in the LRS, suggesting that variability is less critical in this state.

In summary, the introduction of dopants enhances the retention behavior of VCM ReRAM devices in both the HRS and LRS. The stabilizing effect is particularly evident in the HRS, where dopants reduce the broadening of current distributions over time, improving long-term data retention. These findings align with experimental results from Kempen et al.27 and provide a strong motivation for further exploration of dopant effects on ReRAM reliability.

III. CONCLUSIONS

This study investigates the influence of dopants on the reliability of VCM ReRAM devices using an advanced 3D KMC simulation model. Two critical reliability metrics, variability and retention, are systematically analyzed.

The results demonstrate that dopants significantly enhance device variability by reducing the frequency of oxygen vacancy-induced current fluctuations. The introduction of dopants increases the signal-to-noise ratio (SNR) through a trapping effect, which stabilizes the oxygen vacancy configuration without altering the type of current fluctuations. Furthermore, the retention behavior of doped devices shows substantial improvement, in the high resistive state (HRS) as well as in the low resistive state (LRS). Doped cells exhibit much more stable current distributions over time, with reduced broadening and slower degradation of the mean current compared to undoped devices. These findings align well with experimental observations reported in the literature, highlighting the potential of dopants to mitigate reliability challenges in VCM ReRAM.

Future experimental investigations are strongly encouraged to validate the simulation predictions and to optimize dopant parameters, such as concentrations used dopant material), for practical impermentation would not only confirm the reliability benefits demonstrated incre, but also provide further insights into the interplay between the oxygen vacancy dynamics, and device performance. ters, such as concentration and energy levels (corresponding to the

See the supplementary material for Figs. S1-S3. Additional information on the read current traces, the SNR worst-case scenario, and HRS retention with drifting behavior can be found in the supplementary material.

ACKNOWLEDGMENTS

This work was supported by the Federal Ministry of Education and Research (BMBF, Germany) in the project NEUROTEC II (Nos. 16ME0398K and 16ME0399). It is based on the Jülich Aachen Research Alliance (JARA-FIT). The authors gratefully acknowledge computing time on the supercomputer JURECA³⁸ at Forschungszentrum Jülich under Grant No. 27525.

AUTHOR DECLARATIONS

Conflict of Interest

The authors have no conflicts to disclose.

Author Contributions

N. Kopperberg: Conceptualization (equal); Data curation (lead); Investigation (lead); Visualization (lead); Writing - original draft (lead). D. Genua Noguera: Data curation (supporting); Investigation (supporting). S. Menzel: Conceptualization (equal); Project administration (lead); Writing - review & editing (lead).

DATA AVAILABILITY

The data that support the findings of this study are openly available in Jülich Data at https://doi.org/10.26165/JUELICH-DATA/H155MZ, Ref. 42.

REFERENCES

- ¹Y. Chen, "ReRAM: History, status, and future," IEEE Trans. Electron Devices **67**, 1420–1433 (2020).
- ²Z. Wang, H. Wu, G. W. Burr, C. S. Hwang, K. L. Wang, Q. Xia, and J. J. Yang, "Resistive switching materials for information processing," Nat. Rev. Mater. 5, 173–195 (2020)
- ³R. Dittmann, S. Menzel, and R. Waser, "Nanoionic memristive phenomena in metal oxides: The valence change mechanism," Adv. Phys. **70**, 155–349 (2021).
- ⁴G. W. Burr, R. M. Shelby, A. Sebastian, S. Kim, S. Kim, S. Sidler, K. Virwani, M. Ishii, P. Narayanan, A. Fumarola, L. L. Sanches, I. Boybat, M. L. Gallo, K. Moon, J. Woo, H. Hwang, and Y. Leblebici, "Neuromorphic computing using non-volatile memory," Adv. Phys.: X 2, 89–124 (2017).
- ⁵D. V. Christensen *et al.*, "2022 roadmap on neuromorphic computing and engineering," Neuromorph. Comput. Eng. **2**, 022501 (2022).
- ⁶K. A. Nirmal, D. D. Kumbhar, A. V. Kesavan, T. D. Dongale, and T. G. Kim, "Advancements in 2D layered material memristors: Unleashing their potential beyond memory," npj 2D Mater. Appl. 8, 83 (2024).
- ⁷M. Lanza, A. Sebastian, W. D. Lu, M. L. Gallo, M.-F. Chang, D. Akinwande, F. M. Puglisi, H. N. Alshareef, M. Liu, and J. B. Roldan, "Memristive technologies for data storage, computation, encryption, and radio-frequency communication," Science 376, eabj9979 (2022).
- ⁸M. Hellenbrand, I. Teck, and J. L. MacManus-Driscoll, "Progress of emerging non-volatile memory technologies in industry," MRS Commun. 14, 1099–1112 (2024).
- ⁹R. Strenz, "Review and outlook on embedded NVM technologies—From evolution to revolution," in *International Memory Workshop (IMW)* (IEEE, 2020), pp. 1–4.
- 10 M. Csontos, Y. Horst, N. J. Olalla, U. Koch, I. Shorubalko, A. Halbritter, and J. Leuthold, "Picosecond time-scale resistive switching monitored in real-time," Adv. Electron. Mater. 9, 2201104 (2023).
 11 M. von Witzleben, S. Wiefels, A. Kindsmüller, P. Stasner, F. Berg, F. Cüppers,
- ¹¹M. von Witzleben, S. Wiefels, A. Kindsmüller, P. Stasner, F. Berg, F. Cüppers, S. Hoffmann-Eifert, R. Waser, S. Menzel, and U. Böttger, "Intrinsic reset speed limit of valence change memories," ACS Appl. Electron. Mater. 3, 5563–5572 (2021).
- ¹²Y. Hou, U. Celano, L. Goux, L. Liu, A. Fantini, R. Degraeve, A. Youssef, Z. Xu, Y. Cheng, J. Kang, M. Jurczak, and W. Vandervorst, "Sub-10 nm low current resistive switching behavior in hafnium oxide stack," Appl. Phys. Lett. 108, 123106 (2016).
- ¹³U. Celano, A. Fantini, R. Degraeve, M. Jurczak, L. Goux, and W. Vandervorst, "Scalability of valence change memory: From devices to tip-induced filaments," AIP Adv. 6, 85009/1–6 (2016).
- ¹⁴B. Govoreanu, G. S. Kar, Y.-Y. Chen, V. Paraschiv, S. Kubicek, A. Fantini, I. P. Radu, L. Goux, S. Clima, R. Degraeve, N. Jossart, O. Richard, T. Vandeweyer, K. Seo, P. Hendrickx, G. Pourtois, H. Bender, L. Altimime, D. J. Wouters, J. A. Kittl, and M. Jurczak, " $10 \times 10 \text{ nm}^2 \text{ Hf/HfO}_x$ crossbar resistive RAM with excellent performance, reliability and low-energy operation," in *International Electron Devices Meeting (IEDM)* (IEEE, 2011), pp. 31.6.1–31.6.4.
- ¹⁵B. J. Choi, A. C. Torrezan, S. Kumar, J. P. Strachan, P. G. Kotula, A. J. Lohn, M. J. Marinella, Z. Li, R. S. Williams, and J. J. Yang, "High-speed and low-energy nitride memristors," Adv. Funct. Mater. 26, 5290–5296 (2016).
- ¹⁶D. Ielmini, Z. Wang, and Y. Liu, "Brain-inspired computing via memory device physics," APL Mater. 9, 050702 (2021).
- 17R. Waser, R. Bruchhaus, and S. Menzel, "Redox-based resistive switching memories," in *Nanoelectronics and Information Technology*, 3rd ed., edited by R. Waser (Wiley-VCH, 2012), pp. 683–710.
- ¹⁸H.-S. P. Wong, H.-Y. Lee, S. Yu, Y.-S. Chen, Y. Wu, P.-S. Chen, B. Lee, F. T. Chen, and M.-J. Tsai, "Metal-oxide RRAM," Proc. IEEE 100, 1951–1970 (2012).

- ¹⁹J.-Y. Chen, C.-W. Huang, C.-H. Chiu, Y.-T. Huang, and W.-W. Wu, "Switching kinetic of VCM-based memristor: Evolution and positioning of nanofilament," Adv. Mater. **27**, 5028–5033 (2015).
- ²⁰S. Menzel and J.-H. Hur, Modeling the VCM- and ECM-Type Switching Kinetics (Wiley-VCH, 2016), pp. 395–436.
- ²¹D. Cooper, C. Bäumer, N. Bernier, A. Marchewka, C. L. Torre, R. E. Dunin-Borkowski, S. Menzel, R. Waser, and R. Dittmann, "Anomalous resistance hysteresis in oxide ReRAM: Oxygen evolution and reincorporation revealed by in situ TEM," Adv. Mater. 29, 1700212 (2017).
- ²²F. Zahoor, F. A. Hussin, U. B. Isyaku, S. Gupta, F. A. Khanday, A. Chattopadhay, and H. Abbas, "Resistive random access memory: Introduction to device mechanism, materials and application to neuromorphic computing," Discov. Nano 18, 2731–9229 (2023).
- 23S. Wiefels, "Reliability aspects in resistively switching valence change memory cells," Ph.D. thesis (Rheinisch-Westfälische Technische Hochschule Aachen, 2021).
 24D. J. Wouters, Y.-Y. Chen, A. Fantini, and N. Raghavan, "Reliability aspects," in Resistive Switching. From Fundamentals of Nanoionic Redox Processes to Memristive Device Applications, edited by D. Ielmini and R. Waser (Wiley-VCH, 2016).
- ²⁵Z. Swaidan, R. Kanj, J. E. Hajj, E. Saad, and F. Kurdahi, "RRAM endurance and retention: Challenges, opportunities and implications on reliable design," in *International Conference on Electronics, Circuits and Systems (ICECS)* (IEEE, 2019), pp. 402–405.
- ²⁶N. Kopperberg, S. Wiefels, K. Hofmann, J. Otterstedt, D. J. Wouters, R. Waser, and S. Menzel, "Endurance of 2 Mbit based BEOL integrated ReRAM," IEEE Access 10, 122696–122705 (2022).
- 27 T. Kempen, R. Waser, and V. Rana, "50x endurance improvement in TaO_x RRAM by extrinsic doping," in *International Memory Workshop (IMW)* (IEEE, 2021), pp. 1–4.
- 28 Y. Y. Chen, R. Roelofs, A. Redolfi, R. Degraeve, D. Crotti, A. Fantini, S. Clima, B. Govoreanu, M. Komura, L. Goux, L. Zhang, A. Belmonte, Q. Xie, J. Maes, G. Pourtois, and M. Jurczak, "Tailoring switching and endurance/retention reliability characteristics of HfO₂/Hf RRAM with Ti, Al, Si dopants," in Symposium on VLSI Technology (IEEE, 2014).
- on VLSI Technology (IEEE, 2014).

 ²⁹H. He, X. Yuan, W. Wu, C. Lee, Y. Zhao, and Z. Liu, "Impact of Al alloying/doping on the performance optimization of HfO₂-based RRAM," Electronics 13, 2384 (2024).
- The Hall Jiang and D. A. Stewart, "Using dopants to tune oxygen vacancy formation in transition metal oxide resistive memory," ACS Appl. Mater. Interfaces 9, 16296–16304 (2017).
- ³¹M. Schie, R. Waser, and R. A. D. Souza, "A simulation study of oxygenvacancy behavior in strontium titanate: Beyond nearest-neighbor interactions," J. Phys. Chem. **118**, 15185–15192 (2014).
- ³²L. Zhao, S.-G. Park, B. Magyari-Köpe, and Y. Nishi, "Dopant selection rules for desired electronic structure and vacancy formation characteristics of TiO₂ resistive memory," Appl. Phys. Lett. **102**, 083506 (2013).
- ³³N. Kopperberg, S. Wiefels, S. Liberda, R. Waser, and S. Menzel, "A consistent model for short-term instability and long-term retention in filamentary oxide-based memristive devices," ACS Appl. Mater. Interfaces 13, 58066–58075 (2021).
- ³⁴N. Kopperberg, D. J. Wouters, R. Waser, S. Menzel, and S. Wiefels, "Accurate evaluation method for HRS retention of VCM ReRAM," APL Mater. **12**, 031112 (2024).
- 35S. Wiefels, N. Kopperberg, K. Hofmann, J. Otterstedt, D. Wouters, R. Waser, and S. Menzel, "Reliability aspects of 28 nm BEOL-integrated resistive switching random access memory," Phys. Status Solidi A 221(22), 2300401 (2023).
- ³⁶E. Abbaspour, "Modeling and simulation of valence-change based resistive switching," Ph.D. thesis (Rheinisch-Westfälische Technische Hochschule Aachen, 2019).
- ³⁷N. Kaiser, Y.-J. Song, T. Vogel, E. Piros, T. Kim, P. Schreyer, S. Petzold, R. Valenti, and L. Alff, "Crystal and electronic structure of oxygen vacancy stabilized rhombohedral hafnium oxide," ACS Appl. Electron. Mater. 5, 754–763 (2023).
- ³⁸Jülich Supercomputing Centre, "JURECA: Data centric and booster modules implementing the modular supercomputing architecture at Jülich supercomputing centre," J. Large-Scale Res. Facil. 7, A182 (2021).

³⁹ E. Voigtman, "Comparison of signal-to-noise ratios," Anal. Chem. 69,

<sup>226–234 (1997).

40</sup> K. Schnieders, C. Funck, F. Cüppers, S. Aussen, T. Kempen, A. Sarantopoulos, R. Dittmann, S. Menzel, V. Rana, S. Hoffmann-Eifert, and S. Wiefels, "Effect of electron conduction on the read noise characteristics in ReRAM devices," APL Mater. 10, 101114 (2022).

⁴¹S. Wiefels, C. Bengel, N. Kopperberg, K. Zhang, R. Waser, and S. Menzel, "HRS instability in oxide based bipolar resistive switching cells," IEEE Trans.

Electron Devices **67**, 4208–4215 (2020). **42**N. Kopperberg, D. Genua Noguera, and S. Menzel (2025). "Replication data for: 3D KMC-based investigation of the influence of dopants on the reliability of VCM ReRAM," Jülich Data.